**Desalination and Water Treatment**
www.deswater.com

doi: 10.1080/19443994.2014.969319

57 (2016) 835–844
January

Taylor & Francis
Taylor & Francis Group

# Solar photocatalytic degradation of phenol by $TiO_2$/AC prepared by temperature impregnation method

Mohamed Gar Alalm[a,*], Ahmed Tawfik[a], Shinichi Ookawara[b]

[a]*Environmental Engineering Department, Egypt-Japan University of Science and Technology (E-Just), New Borg El Arab City 21934, Egypt, Tel./Fax: +20 34599520; emails: mohamed.alkalla@ejust.edu.eg (M. Gar Alalm), ahmed.tawfik@ejust.edu.eg (A. Tawfik)*
[b]*Graduate School of Engineering and Science, Department of Chemical Engineering, Tokyo Institute of Technology, O-okayama, Meguro-ku, Tokyo 152-8552, Japan, Tel./Fax: +81 3 5734 3692; email: sokawara@chemeng.titech.ac.jp (S. Ookawara)*

Received 6 April 2014; Accepted 19 September 2014

## ABSTRACT

Solar photocatalytic degradation of phenol by $TiO_2$ (p25), which was immobilized on powdered activated carbon ($TiO_2$/AC) by temperature impregnation method, was investigated. Solar compound parabolic collectors reactor with a capacity of 4.0 L was used. Characterization of $TiO_2$/AC by Brunauer–Emmett–Teller analysis, Fourier transform infrared spectroscopy, and scanning electron microscope revealed successful impregnation of $TiO_2$ particles on activated carbon (AC). Fifty three percent degradation of phenol was recorded at irradiation time of 30 min and increased up to 80% after 150 min using $TiO_2$. This was not the case for $TiO_2$/AC, where the phenol was rapidly removed by a value of 40% within 15 min and complete degradation of phenol was attained at illumination time of 120 min. This indicates that immobilization of $TiO_2$ on AC is very effective for phenol degradation. Moreover, in $TiO_2$/AC photocatalysis, the presence of aromatic intermediates (catechol, hydroquinone, and p-benzoquinone) was relatively lower as compared to $TiO_2$ photocatalysis. However, $TiO_2$/AC photocatalysis of phenol degradation is strongly affected by pH values and dosage of the catalyst, i.e. complete degradation of phenol was occurred at pH value of 5.3 and dosage of 1.2 g/L. The photocatalytic degradation of phenol by $TiO_2$/AC followed the pseudo-first-order kinetic according to Langmuir–Hinshelwood model. Costs estimation of full-scale solar oxidation plant with life time of 20 years was assessed. The results showed that complete removal of phenol using $TiO_2$/AC costs 3.19 €/$m^3$.

*Keywords:* Photocatalysis; $TiO_2$/AC; Phenol; Activated carbon; Compound parabolic collectors

## 1. Introduction

Phenol is found in the wastewater generated from several industries such as polymerization inhibitors, petrochemical, paint, textile, oil refineries, photographic chemicals, antioxidants, and flavoring agents [1,2]. Discharge of phenol-rich wastewater into water streams in Egypt seriously causes environmental problems and harmful to human beings [3,4]. Therefore, wastewater containing phenolic compounds should be

---

*Corresponding author.

treated prior discharging into the environment. Traditionally, the attention received by conventional biological treatment far exceeds that of other treatment processes, in part due to its low cost and versatility. However, the presence of toxic and/or inhibitory chemicals dramatically reduces the viability of biological processes [5]. Advanced oxidation processes (AOPs) have been realized as particularly efficient technologies for phenol and pesticides degradation [3,6,7]. In AOPs powerful reactive species like hydroxyl radicals (·OH) are generated by specific chemical reactions in aqueous solutions [8]. (·OH) is able to destroy even the most recalcitrant organic molecules and convert them into relatively benign and less persistent end products such as $CO_2$, $H_2O$, and inorganic ions [9]. Among AOPs processes, heterogeneous photocatalysis using artificial or solar irradiation has been recognized to be effective for the degradation of several types of phenolic compounds [10]. In the heterogeneous UV/$TiO_2$ technique, the ultraviolet light ($\lambda < 400$ nm) is utilized as an energy source and $TiO_2$ playing as a semiconductor photocatalyst [11–13]. $TiO_2$ is distinctive with high surface area, good particle size distribution, high chemical stability, and the possibility of using sunlight as a source of irradiation [14]. In the photocatalysis oxidation process, the photons with energies bigger than the band-gap energy cause the excitation of valence band (VB) electrons which then enhance the reactions with organic pollutants [15–17]. Illumination of the catalyst active surface with sufficient energy contributes to the creation of a positive hole ($h^+$) in the VB and an electron ($e^-$) in the conduction band. The positive hole oxidizes either the organic pollutant or $H_2O_2$ to induce hydroxyl radicals [18].

Several attempts have been made to load the $TiO_2$ nanoparticles on different supports to enhance the photocatalytic activity and make the separation of treated effluent easier [19–21]. Coating surfaces with $TiO_2$ have relatively low photocatalytic efficiency because of low particles dispersion and limited mass transfer between the pollutants and the semiconductor [17,22]. Many researchers have shown that the semiconductor can be more effective and easily separated from the effluent if it was supported on adsorbent surface such as powdered activated carbon (PAC) [16,23,24].

Activated carbon (AC) is not reported to have photocatalytic activity but it improves the photocatalytic activity of $TiO_2$ and this is due to the increased adsorption of contaminants on $TiO_2$/AC. Increased adsorption leads to higher concentration of contaminants around $TiO_2$ [25]. PAC has a well-developed pore structure, very large surface area, and high adsorption capacity and is widely used as an adsorbent for organic and inorganic substances. AC in the $TiO_2$/AC catalysts can act as a center where organic molecules can adsorb before transferring to the decomposition center [25].

The aim of the present research is to evaluate the effect of $TiO_2$/AC photocatalyst prepared by temperature impregnation method for solar photocatalytic degradation of phenol. Emphasis is also afforded for investigating the fate of intermediate products from the photocatalysis process. Catalyst characterization and parameters affecting the photo degradation activity such as pH and catalyst loading were studied. In addition, the pseudo-first-order kinetic reaction was tested according to Langmuir–Hinshelwood model.

## 2. Materials and methods

### 2.1. Chemicals

Phenol and intermediate ring compounds such as catechol, hydroquinone, and p-benzoquinone were purchased from Merck (Germany) with purities ≥99% and used as received. The $TiO_2$ (p25) was obtained from Acros. PAC was purchased from Adwic.

### 2.2. Catalyst preparation

The $TiO_2$/AC catalyst was prepared according to the high temperature impregnation method described by El-Sheikh et al. [26]. 5 g of $TiO_2$ was heated and stirred with 100 mL of distilled water until reach 70°C. Amount of PAC was added with ratio 1:2 and 1:3 of $TiO_2$ to AC and the stirring continued for 90 min under the same temperature. At the beginning of stirring, both white color of $TiO_2$ and black color of carbon were apparently noticed. During the mixing period, the black and white colors disappeared and one gray color produced. This was considered as an indication of interaction between the AC and $TiO_2$. The solution was kept at rest for 15 min for precipitation of suspended materials, and then the supernatant was decanted and the solid was dried at 200°C for 12 h.

### 2.3. Photocatalysis experiments

Photocatalysis experiments were carried out using compound parabolic collectors (CPC) reactor placed in Borg Alarab City, Egypt (latitude 30° 52´, longitude 29° 35´) on the roof of environmental engineering department. The photoreactor module

(0.36 $m^2$) consists of six borosilicate tubes with diameter 1 inch and length 75 cm mounted on a curved polished aluminum reflector sheet with radius of curvature 9.2 cm. The module is tilted by an angle equal to the position latitude ≈30˚, where the sunlight is perpendicular to the reactor. The parabolic reflection surface insures that the reaction tubes are exhibited to light. The borosilicate tubes are transparent for light with wavelength > 275 nm which certainly allow UVA (315–400 nm) and UVB (280–315 nm) to reach the solution. UVC ranged from 100 to 280 nm is naturally blocked from reaching the earth surface by the atmosphere and ozone layer. Accordingly, all the measured UV light is considered to reach the solution inside the reaction tubes. The reaction time of all experiments is normalized to UV intensity of 30 $W/m^2$ according to Eqs. (1) and (2). Based on the module area of 0.36 $m^2$ and the reactor irradiated volume of 2.2 L, the solution is irradiated by 4.91 W/L.

The reactor is connected at both the inlet and outlet with a tank containing the phenol solution as a sole substrate. The substrate was continuously circulated in a closed cycle. A schematic diagram of the experimental setup is shown in Fig. 1. The reactor was initially fed with 4 L of the 100 mg/L phenol solution. To evaluate the effect of $TiO_2$ immobilization on AC, both $TiO_2$ and $TiO_2$/AC were used as catalysts. The pH was adjusted in the range of 2.7–11.4 by few drops of $H_2SO_4$ or NaOH. The effect of $TiO_2$/AC dosage was investigated by varying the dosage from 0.4 to 2 g/L. To evaluate the adsorption of phenol into the catalysts, the first 30 min was spent only for adsorption process by mechanical mixing in the tank without turning on the recirculation pump. The solar irradiation was measured by Met one Portable Weather Station (Model Number 466A) installed in the same location. The normalized illumination time ($t_{30w}$) was used to compare between photocatalytic experiments instead of exposition time ($t$). The normalized illumination time was calculated by the following equations [11,27]:

$$t_{30\mathrm{w,n}} = t_{30\mathrm{w,n}-1} + \Delta t_{\mathrm{n}} \left(\frac{\mathrm{UV}}{30}\right) \left(\frac{V_{\mathrm{i}}}{V_{\mathrm{t}}}\right) \tag{1}$$

$$\Delta t_{\mathrm{n}} = t_{\mathrm{n}} - t_{\mathrm{n}-1} \tag{2}$$

where $t_n$: the experimental time for each sample, UV: the average solar ultraviolet radiation ($W/m^2$) measured during $\Delta t_n$, $t_{30W}$: the normalized illumination time, which refers to a constant solar UV power of 30 $W/m^2$ (typical solar UV power on a perfectly sunny day around noon), $V_t$: the total reactor volume, and $V_i$: the total irradiated volume.

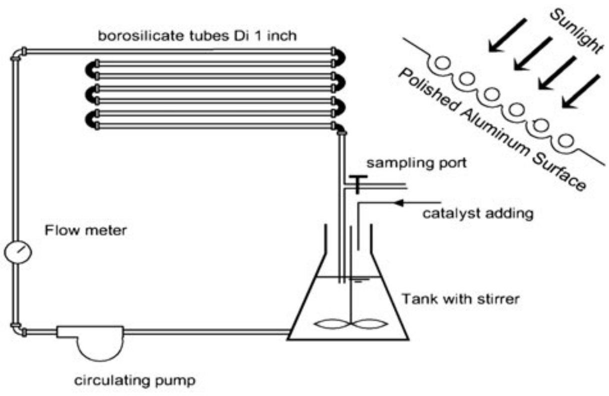

Fig. 1. Schematic diagram of solar CPCs reactor.

### 2.4. Analytical methods

Phenol and oxidation intermediate ring compounds (catechol, hydroquinone, and p-benzoquinone) were quantified by Shimadzu HPLC by C-18 phenomenex reverse phase column, degasser (20A5), pump (LC-20AT), and prominences diode array detector (SPD-M20A). The samples were filtered by micro syringe filters (0.2 μm). The mobile phase was a mixture of ultrapure water/methanol/ acetic acid with volumetric percent ratio of 79.2:19.8:1.0. The flow rate of the mobile phase was 0.8 mL/min. The monitoring wave lengths were chosen as 270, 276, 290, and 245 nm for phenol, catechol, hydroquinone, and p-benzoquinone, respectively. For characterization of catalysts, Fourier transform infrared spectroscopy (FTIR) spectra were recorded on a VERTEX 70 spectrometer over the wave number range 3,800–400 $cm^{-1}$using KBr pellets for sample preparation. Scanning electron microscope (SEM) images were obtained with a JEOL 611. Surface area and pore size were determined by Brunauer–Emmett–Teller (BET) analysis using Belsorp-max automated apparatus using liquid $N_2$ adsorption at temperature of 77 K.

## 3. Results and discussion

### 3.1. Characterization of PAC and TiO2/AC

BET analysis data are summarized in Table 1. The specific surface area was decreased from 1,322.7 to 846.4 $m^2/g$ by impregnation of $TiO_2$ into AC, which confirms the deposition of $TiO_2$ on the external surface

Table 1
BET analysis of AC and $TiO_2$/AC

| Parameter | AC | $TiO_2$/AC |
|---|---|---|
| Specific surface area $S_{BET}$ ($m^2$/g) | 1,322.7 | 846.4 |
| Total pore volume ($cm^3$/g) | 0.8638 | 0.7994 |
| Mean pore diameter (nm) | 2.61 | 3.78 |

of AC. The effect of high temperature calcinations that induce the formation of anatase $TiO_2$ on the surface and pores of AC is the main reason for reducing the surface area of the $TiO_2$/AC [26]. Likely, total pore volume was slightly decreased from 0.8638 for AC to 0.7994 $cm^3$/g for $TiO_2$/AC. However, mean pore diameter of AC and $TiO_2$/PAC was increased from 2.61 to 3.78 nm, respectively. Both processes are mainly occurred due to the partial pore collapse and shrinkage after impregnation at high temperature that may cause changes in pore structure from micropores to mesopores [28]. In addition, the larger pores may be due to the formation of inter-agglomeration particles [29].

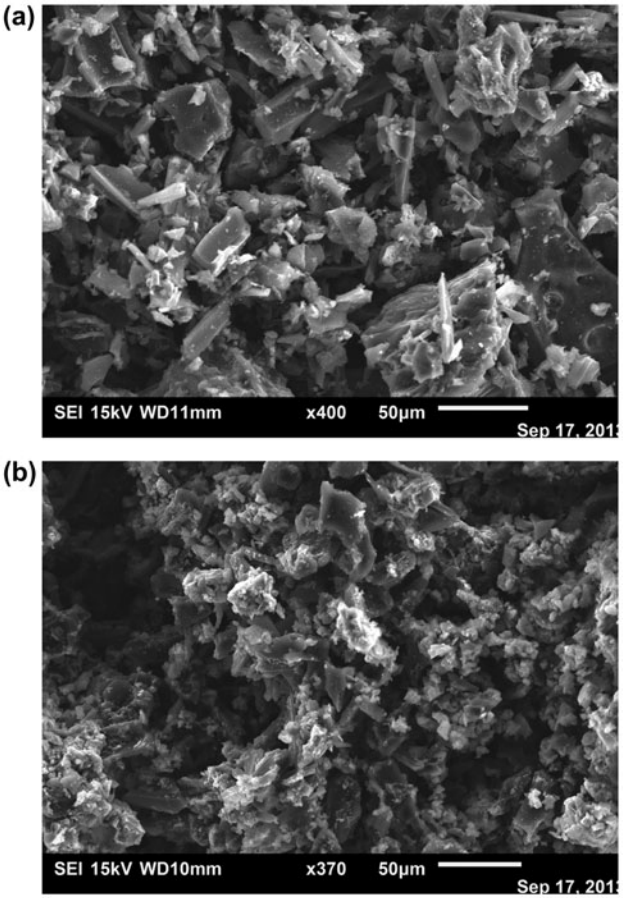

Fig. 2. SEM of (a) naked AC and (b) $TiO_2$/AC.

SEM images of naked PAC and the composite of $TiO_2$/AC are shown in Fig. 2(a) and (b). The surface of naked AC is clear and the particulates have irregular shapes (Fig. 2(a)). Moreover, the surface of AC particulates is rough with heterogeneous pores, which certainly indicates a good possibility for $TiO_2$ to be entrapped and adsorbed onto the surface of the pores of AC. For the $TiO_2$/AC, the SEM image (Fig. 2(b)) indicates that $TiO_2$ particles are uniformly adsorbed on the surface of AC. The supported $TiO_2$ which appears in image by gray color covered most of the surface of AC, and also it is reported that some of $TiO_2$ could deposit in the mesopores and macrospores of AC [24]. Since the photocatalysis process strongly depends on light intensity, deposition of $TiO_2$ on the external surface of PAC will undoubtedly provide more chance to be exhibited to light and subsequently improved the degradation process. Moreover, a high content $TiO_2$ on the external surface of AC is favored to enhance the photocatalytic activity.

FTIR spectra of AC and $TiO_2$/AC are illustrated in Fig. 3. The spectrums revealed that immobilization of $TiO_2$ on the AC produced a broad peak from 400 to 800 $cm^{-1}$ which could be attributed to the existence of bulk Titania framework [12]. This indicated a good interaction between the AC surface and titanium dioxide. Also, the peak at 1,650 $cm^{-1}$ assigned to –OH vibration was shifted to 1,585 $cm^{-1}$. A new peak at 1,165 $cm^{-1}$ was appeared in the spectrum of $TiO_2$/AC. This is mainly a result of the Ti–O–C band owing to the electron affinity of carbon when using hydrothermal methods in preparation of $TiO_2$/AC [23]. The peak at 2,382 $cm^{-1}$ which is assigned to O–H stretching [30] was

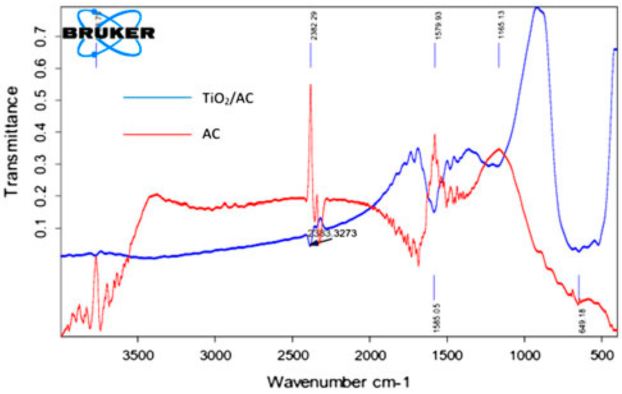

Fig. 3. FTIR spectra of AC and $TiO_2$/AC.

minimized after $TiO_2$ impregnation. Moreover, the band at 3,400 cm$^{-1}$ that assigned to –OH stretching [31] was disappeared in $TiO_2$/AC spectra.

### 3.2. Evaluation of photocatalytic activity

Adsorption and photocatalytic degradation efficiency of phenol using $TiO_2$ and $TiO_2$/AC are shown in Fig. 4. It could be observed that there is no significant removal of phenol by the adsorption on the $TiO_2$, while about 10% of phenol was adsorbed on the $TiO_2$/AC surface because of the surface area and adsorption capacity of PAC [19]. In $TiO_2$photocatalytic process, 53% degradation of phenol was recorded at the first 30 min and increased up to 80% after 150 min. This decreasing in reaction rate was due to the consuming most of $TiO_2$ in the first 30 min. This was not the case for $TiO_2$/AC, where the phenol was rapidly removed by a value of 40% within 15 min and complete degradation of phenol was attained at irradiation time of 120 min. Although, AC has no photocatalytic activity, the enhanced photocatalytic performance of $TiO_2$/AC was apparently attributed to the increasing of adsorption of phenol on the surface of AC which indeed leads to more phenol existence around $TiO_2$ adhered on AC. Therefore, it is concluded that the phenol degradation was achieved through a synergistic mechanism of adsorption and $TiO_2$ photocatalysis reaction [24]. Nevertheless, phenol oxidation degradation using photocatalysis process ($TiO_2$/AC) is accompanied with evolution of aromatic intermediates such as benzoquinone, catechol (benzene-1,2-diol), hydroquinone (1,4-Dihydroxybenzene) [32]. As shown in Fig. 4, the main intermediates generated here are hydroquinone and catechol, while benzoquinone was slightly appeared. The formation of hydroquinone and catechol can be attributed to the activation of phenol molecules by reaction with an OH radical [33].The $^{\cdot}OH$ radical attacks the phenyl ring of the phenol yielding catechol, 1,2,3-benzenetriol, and hydroquinone. Furthermore, the phenyl rings disintegrate to produce malonic acid. Afterward, short-chain organic acids, such as maleic, oxalic, acetic, formic 3-hydroxy propyl carboxylic acid, 2-hydroxy propanal, 2-hydroxy-ethanoic acid glycol acid, are oxidized to produce $CO_2$ and $H_2O$. $H^{\cdot}$ produced during the attack of bonds by $^{\cdot}OH$ is reported to be an important active free radical in the degradation process. During the process, H+ or $H^{\cdot}$ is scavenged by oxygen to form $HO_2^{\cdot}$ radicals, which eventually convert to $^{\cdot}OH$ radicals. Therefore, the principal reaction leading to organics decomposition would be the one with $^{\cdot}OH$ radicals [34].

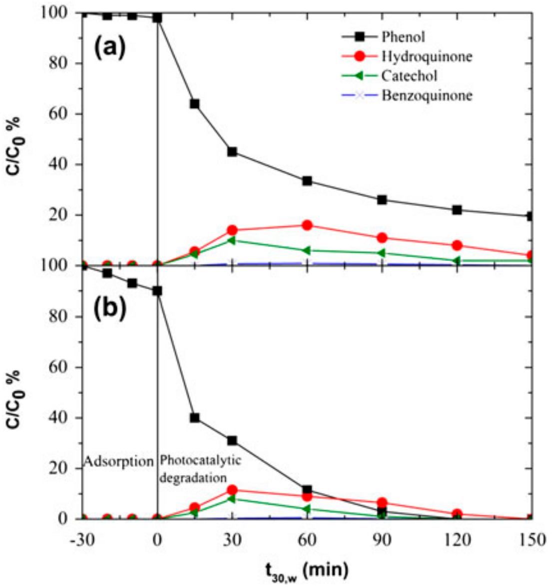

Fig. 4. Photocatalytic degradation of phenol (a) $TiO_2$ and (b) $TiO_2$/AC.

In $TiO_2$ photocatalysis, hydroquinone gradually increased in the first 60 min to reach 16 mg/L, while the maximum formation of catechol was 10.5 mg/L after 30 min. With the decreasing of phenol concentration, the aromatic intermediates are also oxidized into carboxylic acids and $CO_2$. Finally, carboxylic acid generated from the oxidation process is converted into $CO_2$ [35]. In $TiO_2$/AC photocatalysis, the presence of aromatic intermediates was relatively lower as compared to $TiO_2$ photocatalysis. Maximum concentration of hydroquinone and catechol was 11.5 and 8 mg/L, respectively, after 30 min of irradiation. It is assumed that a portion of intermediates is adsorbed on the surface of AC and rapidly oxidized to carboxylic acids and $CO_2$. Based on these results immobilization of $TiO_2$ on AC is very effective for phenol degradation. However, pH values and dosage of $TiO_2$/AC should be optimized.

### 3.3. Factors affecting on photocatalytic oxidation process using $TiO_2$/AC

#### 3.3.1. Effect of initial pH

The pH has a significant influence on both adsorption and photocatalytic degradation process. Therefore, the effect of initial pH was investigated in acidic and alkaline conditions. The degradation of phenol was improved under acidic pH (Fig. 5(a)). The optimal solution pH was 5.3 in which a complete degradation of phenol was achieved after 120 min of irradiation.

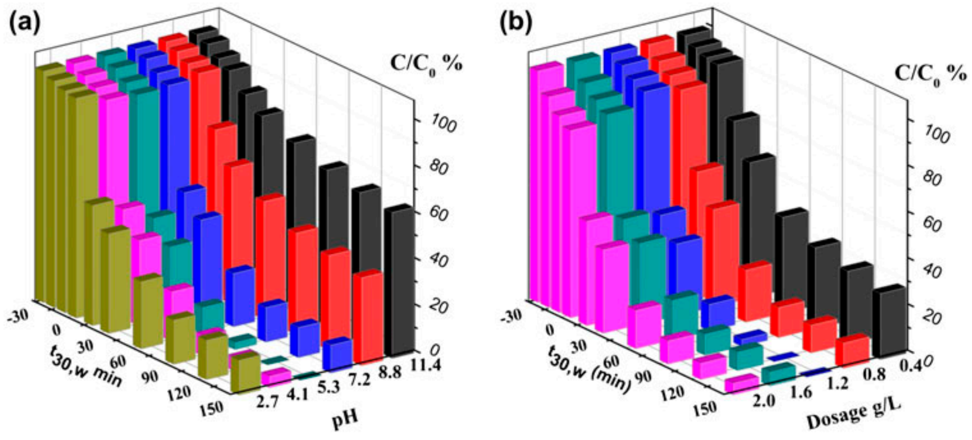

Fig. 5. Parameters effect on photocatalytic degradation (a) effect of pH and (b) effect of $TiO_2$/AC dosage.

Further rising of the initial pH led to a decrease in degradation efficiency of phenol. These results correspond closely to other similar reported work [12,36,37]. At optimum pH value of 5.3, the electrostatic attraction force between phenol molecules and positively charged $TiO_2$ resulted in maximum oxidation activity, and thus led to high degradation efficiency of phenol. At higher pH value, the phenol molecules have negative charges, which led to repulsion with $TiO_2$ particulates and decrease the photocatalytic activity [37]. Besides, adjusting the pH by NaOH is reported to create a competition on adsorption on the surface of $TiO_2$ between the $Na^+$ions and $OH^-$ ions with the phenol anions, which resulted in a lower photocatalytic degradation efficiency [4].

The effect of pH on degradation of phenol assisted by the semiconductor oxides is influenced by the acid–base equilibrium governing the surface chemistry of metal oxides in water as shown in the following reactions:

$$\text{At pH} < P_{zc} \quad \text{TiOH} + \text{H}^+ \rightarrow \text{TiOH}_2^+ \tag{3}$$

$$\text{At pH} > P_{zc} \quad \text{TiOH} + \text{OH}^- \rightarrow \text{TiO}^- + \text{H}_2\text{O} \tag{4}$$

where $P_{zc}$ is the zero point of charge of the semiconductor [38]. It is defined as the pH at which the surface of an oxide is uncharged. The point of zero charge of the $TiO_2$ (p25) is reported to be about 6.25 [39,40]. The effect of pH on the photooxidation activity could be explained in terms of electrostatic interaction between the active semiconductor sites and the substrate molecules [18]. The interaction could be expected to affect the encounter probability of the resulted hydroxyl radical with the molecules. It is stated that the overall reaction would be improved or restrained depending on whether attractive or repulsive forces prevail, respectively [41]. In addition, the adsorption of phenol on the AC surface is enhanced in acidic condition [42,43]. Increasing the amount of phenol adsorbed on the surface of AC improve the interaction between $TiO_2$ and phenol molecules.

### 3.3.2. Effect of $TiO_2$/AC dosage

The effect of dosage of $TiO_2$/AC on phenol degradation is shown in Fig. 5(b). The results revealed that photocatalytic degradation efficiency is improved with increasing the dosage of $TiO_2$/AC from 0.4 to 1.2 g/L. This can be attributed to the increasing of active sites by providing a higher amount of catalyst, which is the semiconductor in the reaction [44]. Consequently, the formation of electron hole pairs on the surface of semiconductor and the high reactive hydroxyl radicals increased, which cause the oxidation of phenol into other intermediates [40]. The optimum dosage of $TiO_2$/AC was 1.2 g/L which achieved a complete degradation of phenol within 120 min of irradiation. Increasing the dosage up to 1.6 and 2.0 g/L declined the degradation efficiency due to the increasing of turbidity in the solution, which detracts the amount of light reaching the semiconductor active sites [34]. Furthermore, increasing the catalyst loading may cause agglomeration of particulates, which decreases the active sites on the semiconductor surface [40].

## 3.4. Degradation kinetics

The Langmuir–Hinshelwood model is usually used to describe the kinetics of photocatalytic degradation of organics in aqueous solutions [45]. It basically relates the degradation rate ($r$) and reactant concentration ($C$) in water at time $t$, which is expressed by the following equation [46]:

$$r = -\frac{\mathrm{d}C}{\mathrm{d}t} = \frac{K_\mathrm{r}K_\mathrm{ad}C}{1 + K_\mathrm{ad}C} \tag{5}$$

where $k_\mathrm{r}$ is the rate constant and $K_\mathrm{ad}$ is the adsorption equilibrium constant. In photocatalysis where the adsorption is relatively weak like and/or the reactant concentration is low, Eq. (5) can be simplified to the pseudo-first-order kinetics with an apparent first-order rate constant $K_\mathrm{app}$ [45]:

$$\ln\left(\frac{C_0}{C}\right) = K_\mathrm{r}K_\mathrm{ad}t = K_\mathrm{app}t \tag{6}$$

where $C_0$ is the initial concentration of phenol. Fig. 6 shows the linear relationship between Ln ($C_0/C$) and irradiation time. $K_\mathrm{app}$ was calculated for $TiO_2$/AC and $TiO_2$ photocatalysis and found to be 0.041 and 0.010, respectively. This result confirms the enhancement of phenol photocatalytic degradation by immobilizing $TiO_2$ on the surface of PAC. Correlation coefficient ($R^2$) was also calculated and found to be 0.980 and 0.903 for $TiO_2$/AC and $TiO_2$ photocatalysis, respectively.

### 3.5. Economic and cost evaluation

The capital and running costs of industrial wastewater treatment facilities are essential to corroborate the prospect of application in a large commercial scale [47]. Estimation of construction and operation costs depends on the design parameters, i.e. irradiation time and dosage of chemicals [48].

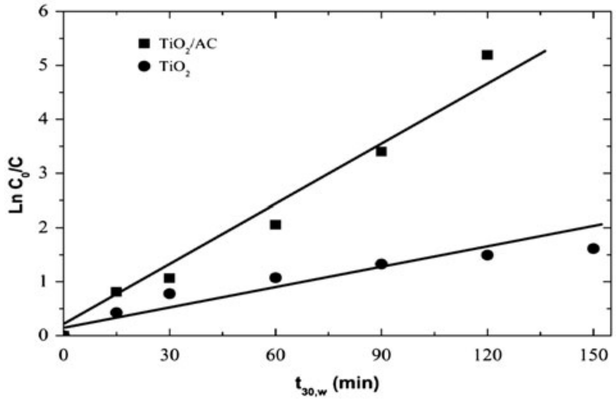

Fig. 6. Kinetic analysis of photocatalytic degradation of phenol.

In this investigation, capital and operation costs of photocatalytic oxidation process of industrial wastewater (30 $m^3$/d) containing phenol (100 ± 20 mg/L) by $TiO_2$ and $TiO_2$/AC were estimated. The capacity ($C$) of the proposed solar photocatalytic reactor is estimated using Eq. (7) [49].

$$C = V_\mathrm{t}\frac{t_\mathrm{t}}{t_\mathrm{w}D} \tag{7}$$

where $V_\mathrm{t}$: volumetric treated wastewater for a year, $t_\mathrm{t}$: operation time for the treatment plant facilities in one batch, $t_\mathrm{w}$: working time per day for wastewater treatment plant, and $D$: the number of working days in a year. Assuming the ratio between batch time and working time is 35% which corresponded to the optimum irradiation time and the average solar UV flux in Egypt. Assuming the ratio of irradiated volume to the total treatment plant volume is 75% and the illumination area of the plant ($A_\mathrm{p}$) is 4.5 $m^2$ based on the volumetric rate of the wastewater.

Amortization costs (AMC) of the investment and operating costs (OC) per $m^3$ of the effluent were considered for cost estimation of the treatment processes. The AMC were calculated taking into consideration the tanks, connections, reflective surface, and the required mechanical equipment. The investment cost per year ($I$) is calculated according to the illumination area of the treatment plant ($A_\mathrm{p}$) and the treatment plant life time ($L$) using Eq. (8) [49]:

$$I = \frac{A_\mathrm{p}C_\mathrm{p}}{L} \tag{8}$$

where $C_\mathrm{p}$: the cost per $m^2$ of the illuminated surface in the plant. A value of 800 €/$m^2$ is considered according to the costs of durable reflection surface, borosilicate tubes, tanks, and other mechanical equipment. The AMC per $m^3$ is calculated by Eq. (9) [50]:

$$\mathrm{AMC} = \frac{I}{V_\mathrm{t}} \tag{9}$$

The OC includes maintenance, the reactants, and the energy consumed. The staff costs are not calculated in this estimation for the simplicity of the calculations. Moreover, the solar photocatalytic reactor is independent on manpower [50]. The maintenance costs are assumed to be 2% of the yearly investment according to previous studies [51,52]. The costs of chemicals including catalysts and pH adjustment reagents are calculated as the concentration ($C_\mathrm{i}$) (kg/$m^3$) multiplied by the unit price ($P_\mathrm{i}$) (€/kg). Prices of chemicals were

Table 2
Costs estimation for $TiO_2$/AC and $TiO_2$ solar photocatalysis

| Catalyst | $TiO_2$ dose (mg/L) | AC dose | Operating costs (€/$m^3$) | Total costs (€/$m^3$) | Removal efficiency (%) |
|---|---|---|---|---|---|
| $TiO_2$/AC | 133 | 267 | 0.81 | 2.33 | 68 |
| $TiO_2$/AC | 267 | 533 | 1.24 | 2.76 | 86 |
| $TiO_2$/AC | 400 | 800 | 1.67 | 3.19 | 100 |
| $TiO_2$ | 200 | 0 | 0.85 | 2.37 | 58 |
| $TiO_2$ | 400 | 0 | 1.31 | 2.83 | 76 |
| $TiO_2$ | 600 | 0 | 1.77 | 3.29 | 88 |
| $TiO_2$ | 800 | 0 | 2.23 | 3.75 | 92 |

taken as the average values from different suppliers inside and outside Egypt. The prices of commercial $TiO_2$ and PAC for industrial use were taken 2.3 €/kg and 0.45 €/kg, respectively. The energy cost (EC) (€/$m^3$) is calculated concerning the required power for pumping the wastewater in the reactor by Eq. (10).

$$EC = \frac{EP_i t_w D}{V_t} \tag{10}$$

where $E$: the power for pumping the effluent from the tank to the reactor and $P_i$: the unit price of energy. It is assumed that the cost of energy is 0.12 €/kw h according to the rates in Egypt. The calculated treatment costs including AMC using $TiO_2$ and $TiO_2$/AC are illustrated in Table 2.

According to the volumetric rate of effluent and reactor life cycle, the AMC was 1.52 €/$m^3$ for all the cases. Table 2 reveals that the variation of OC mainly depends on the type and dosage of the catalyst. Moreover, using $TiO_2$/AC was more economic than using $TiO_2$ concerning the achieved removal efficiency. For instance, the maximum removal efficiency of phenol by $TiO_2$/AC was 100% which costs 3.19 €/$m^3$. On the other hand, the maximum removal efficiency by TiO2 was 92% which costs 3.75 €/$m^3$.

## 4. Conclusions

Photocatalytic degradation of phenol using titanium dioxide ($TiO_2$-p25) as a semiconductor vs. $TiO_2$-p25 immobilized on PAC was investigated. Characterization of $TiO_2$/AC by FTIR revealed successful impregnation of $TiO_2$ on PAC. This was also confirmed by SEM images and BET analysis. Complete degradation of phenol was occurred using$TiO_2$/PAC within 120 min of irradiation. This was not the case for photocatalysis process by TiO2, where 80% of phenol was removed at 150 min of irradiation. This strongly indicates that the immobilization of $TiO_2$ on the PAC significantly improved not only the removal of phenol but also accelerate the reaction rate. Moreover, the phenolic degradation products in the treated effluent in terms of hydroquinone, catechol, and benzoquinone were quite low in $TiO_2$/AC. However, the photocatalytic activity of $TiO_2$/AC was pH and dosage dependant. The optimum pH and dosage of $TiO_2$/AC was 5.3 and 1.2 g/L, respectively. The photocatalytic degradation of phenol by $TiO_2$/AC followed the pseudo-first-order kinetic according to Langmuir–Hinshelwood model. Costs estimation of full-scale plant revealed that $TiO_2$/AC is more economic than $TiO_2$. Based on these results it is recommended to use $TiO_2$ immobilized on ACAC for removal of phenol from industrial liquid effluents.

## Acknowledgments

The first author is grateful for the Egyptian Ministry of Higher Education which provided him a full scholarship and for *Japan International Cooperation Agency* (JICA) for providing all the facilities to participate in this work.

## References

[1] O.B. Ayodele, J.K. Lim, B.H. Hameed, Degradation of phenol in photo-Fenton process by phosphoric acid modified kaolin supported ferric-oxalate catalyst: Optimization and kinetic modeling, Chem. Eng. J. 197 (2012) 181–192, doi: 10.1016/j.cej.2012.04.053.

[2] B. Iurascu, I. Siminiceanu, D. Vione, M.A. Vicente, A. Gil, Phenol degradation in water through a heterogeneous photo-Fenton process catalyzed by Fe-treated laponite, Water Res. 43 (2009) 1313–1322, doi: 10.1016/j.watres.2008.12.032.

[3] G.C. Yang, Y. Long, Removal and degradation of phenol in a saturated flow by in situ electrokinetic remediation and Fenton-like process, J. Hazard. Mater. 69 (1999) 259–271.

[4] S. Bekkouche, M. Bouhelassa, N.H. Salah, F.Z. Meghlaoui, Study of adsorption of phenol on titanium oxide ($TiO_2$), Desalination 166 (2004) 355–362, doi: 10.1016/j.desal.2004.06.090.

[5] H. Kusic, N. Koprivanac, A.L. Bozic, I. Selanec, Photo-assisted Fenton type processes for the degradation of phenol: A kinetic study, J. Hazard. Mater. 136 (2006) 632–644, doi: 10.1016/j.jhazmat.2005.12.046.

[6] T. Olmez-Hanci, I. Arslan-Alaton, Comparison of sulfate and hydroxyl radical based advanced oxidation of phenol, Chem. Eng. J. 224 (2013) 10–16, doi: 10.1016/j.cej.2012.11.007.

[7] K.C. Namkung, A.E. Burgess, D.H. Bremner, H. Staines, Advanced Fenton processing of aqueous phenol solutions: A continuous system study including sonication effects, Ultrason. Sonochem. 15 (2008) 171–176, doi: 10.1016/j.ultsonch.2007.02.009.

[8] M. Gar Alalm, A. Tawfik, Fenton and solar photo-Fenton oxidation of industrial wastewater containing pesticides, 17th Int. Water Technol. Conf. 2 (2013) 5–7.

[9] M.M. Ballesteros Martín, J.A. Sánchez Pérez, J.L. Casas López, I. Oller, S. Malato Rodríguez, Degradation of a four-pesticide mixture by combined photo-Fenton and biological oxidation, Water Res. 43 (2009) 653–660, doi: 10.1016/j.watres.2008.11.020.

[10] Y. Xu, Y. Zhuang, X. Fu, New insight for enhanced photocatalytic activity of $TiO_2$ by doping carbon nanotubes: A case study on degradation of benzene and methyl orange, J. Phys. Chem. C. 114 (2010) 2669–2676.

[11] S. Malato, J. Blanco, J. Cáceres, A.R. Fernández-alba, Photocatalytic treatment of water-soluble pesticides by photo-Fenton and $TiO_2$ using solar energy, Cat. Today. 76 (2002) 209–220.

[12] A. García, J. Matos, Photocatalytic activity of $TiO_2$ on activated carbon under visible light in the photodegradation of phenol, Open Mater. Sci. J. 4 (2010) 2–4.

[13] K.S. Yao, J.J. Hsu, C.Y. Chang, Study on the photocatalytic degradation of wastewater under the optimal preparation of the activated carbon supported $TiO_2$ thin film, Adv. Mater. Res. 356–360 (2011) 313–317, doi: 10.4028/www.scientific.net/AMR.356-360.313.

[14] J.C. Garcia, J.L. Oliveira, A.E.C. Silva, C.C. Oliveira, J. Nozaki, N.E. de Souza, Comparative study of the degradation of real textile effluents by photocatalytic reactions involving $UV/TiO_2/H_2O_2$ and $UV/Fe^{2+}/H_2O_2$ systems, J. Hazard. Mater. 147 (2007) 105–110, doi: 10.1016/j.jhazmat.2006.12.053.

[15] M.V. Phanikrishna Sharma, V. Durga Kumari, M. Subrahmanyam, $TiO_2$ supported over SBA-15: An efficient photocatalyst for the pesticide degradation using solar light, Chemosphere 73 (2008) 1562–1569, doi: 10.1016/j.chemosphere.2008.07.081.

[16] J. Matos, A. Garcia, T. Cordero, J.-M. Chovelon, C. Ferronato, Eco-friendly $TiO_2$–AC photocatalyst for the selective photooxidation of 4-chlorophenol, Catal. Lett. 130 (2009) 568–574, doi: 10.1007/s10562-009-9989-8.

[17] M. Hinojosa-Reyes, S. Arriaga, L.A. Diaz-Torres, V. Rodríguez-González, Gas-phase photocatalytic decomposition of ethylbenzene over perlite granules coated with indium doped $TiO_2$, Chem. Eng. J. 224 (2013) 106–113, doi: 10.1016/j.cej.2013.01.066.

[18] E.S. Elmolla, M. Chaudhuri, Photocatalytic degradation of amoxicillin, ampicillin and cloxacillin antibiotics in aqueous solution using $UV/TiO_2$ and $UV/H_2O_2/TiO_2$ photocatalysis, Desalination 252 (2010) 46–52, doi: 10.1016/j.desal.2009.11.003.

[19] X. Lu, J. Jiang, K. Sun, D. Cui, Applied surface science characterization and photocatalytic activity of $Zn^{2+}$–$TiO_2$/AC composite photocatalyst, Appl. Surf. Sci. 258 (2011) 1656–1661, doi: 10.1016/j.apsusc.2011.09.042.

[20] M.J. Sampaio, C.G. Silva, A.M.T. Silva, V.J.P. Vilar, R.A.R. Boaventura, J.L. Faria, Photocatalytic activity of $TiO_2$-coated glass raschig rings on the degradation of phenolic derivatives under simulated solar light irradiation, Chem. Eng. J. 224 (2013) 32–38, doi: 10.1016/j.cej.2012.11.027.

[21] P.-S. Yap, T.-T. Lim, M. Srinivasan, Nitrogen-doped $TiO_2$/AC bi-functional composite prepared by two-stage calcination for enhanced synergistic removal of hydrophobic pollutant using solar irradiation, Catal. Today 161 (2011) 46–52, doi: 10.1016/j.cattod.2010.09.024.

[22] C. Zhu, X. Wang, Q. Huang, L. Huang, J. Xie, C. Qing, T. Chen, Removal of gaseous carbon bisulfide using dielectric barrier discharge plasmas combined with $TiO_2$ coated attapulgite catalyst, Chem. Eng. J. 225 (2013) 567–573, doi: 10.1016/j.cej.2013.03.107.

[23] X. Zhang, L. Lei, Effect of preparation methods on the structure and catalytic performance of $TiO_2$/AC photocatalysts, J. Hazard. Mater. 153 (2008) 827–833, doi: 10.1016/j.jhazmat.2007.09.052.

[24] X. Wang, Y. Liu, Z. Hu, Y. Chen, W. Liu, G. Zhao, Degradation of methyl orange by composite photocatalysts nano-$TiO_2$ immobilized on activated carbons of different porosities, J. Hazard. Mater. 169 (2009) 1061–1067, doi: 10.1016/j.jhazmat.2009.04.058.

[25] T.S. Jamil, M.Y. Ghaly, N.A. Fathy, T.A. Abd el-halim, L. Österlund, Enhancement of $TiO_2$ behavior on photocatalytic oxidation of MO dye using $TiO_2$/AC under visible irradiation and sunlight radiation, Sep. Purif. Technol. 98 (2012) 270–279, doi: 10.1016/j.seppur.2012.06.018.

[26] A.H. El-Sheikh, A.P. Newman, H. Al-Daffaee, S. Phull, N. Cresswell, S. York, Deposition of anatase on the surface of activated carbon, Surf. Coat. Technol. 187 (2004) 284–292, doi: 10.1016/j.surfcoat.2004.03.012.

[27] M. Lapertot, C. Pulgarín, P. Fernández-Ibáñez, M.I. Maldonado, L. Pérez-Estrada, I. Oller, W. Gernjak, S. Malato, Enhancing biodegradability of priority substances (pesticides) by solar photo-Fenton, Water Res. 40 (2006) 1086–1094, doi: 10.1016/j.watres.2006.01.002.

[28] N.M. Mohammad, A. Behnajady, M.E. Alamdari, Investigation of the effect of heat treatment process on characteristics and photocatalytic activity of $TiO_2$-UV100 nanoparticles, Environ. Prot. Eng. 39 (2013) 33–46, doi: 10.5277/EPE130103.

[29] A. Ishihara, T. Hashimoto, H. Nasu, Large mesopore generation in an amorphous silica-alumina by controlling the pore size with the gel skeletal reinforcement and its application to catalytic cracking, Catalysts 2 (2012) 368–385, doi: 10.3390/catal2030368.

[30] A. Kumar, B. Prasad, I.M. Mishra, Isotherm and kinetics study for acrylic acid removal using powdered activated carbon, J. Hazard. Mater. 176 (2010) 774–783, doi: 10.1016/j.jhazmat.2009.11.102.

[31] S.X. Liu, X.Y. Chen, X. Chen, A $TiO_2$/AC composite photocatalyst with high activity and easy separation prepared by a hydrothermal method, J. Hazard. Mater. 143 (2007) 257–263, doi: 10.1016/j.jhazmat.2006.09.026.

[32] E.E. Bamuza-pemu, E.M.N. Chirwa, Profile of aromatic intermediates of titanium dioxide mediated degradation of phenol, Chem. Engin. Trans. 35 (2013) 1333–1338, doi: 10.3303/CET1335222.

[33] Z. Wang, W. Cai, X. Hong, X. Zhao, F. Xu, C. Cai, Photocatalytic degradation of phenol in aqueous nitrogen-doped $TiO_2$ suspensions with various light sources, Appl. Catal., B 57 (2005) 223–231, doi: 10.1016/j.apcatb.2004.11.008.

[34] S. Ahmed, M.G. Rasul, W.N. Martens, R. Brown, M.A. Hashib, Heterogeneous photocatalytic degradation of phenols in wastewater: A review on current status and developments, Desalination 261 (2010) 3–18, doi: 10.1016/j.desal.2010.04.062.

[35] J. Moreira, B. Serrano, A. Ortiz, H. de Lasa, A unified kinetic model for phenol photocatalytic degradation over $TiO_2$ photocatalysts, Chem. Eng. Sci. 78 (2012) 186–203, doi: 10.1016/j.ces.2012.04.033.

[36] Y. Ma, N. Gao, W. Chu, C. Li, Removal of phenol by powdered activated carbon adsorption, Front. Environ. Sci. Eng. 7 (2013) 158–165, doi: 10.1007/s11783-012-0479-7.

[37] S.-M. Lam, J.-C. Sin, A.R. Mohamed, Parameter effect on photocatalytic degradation of phenol using $TiO_2$-P25/activated carbon (AC), Korean J. Chem. Eng. 27 (2010) 1109–1116, doi: 10.1007/s11814-010-0169-8.

[38] N. Daneshvar, S. Aber, Photocatalytic degradation of the insecticide diazinon in the presence of prepared nanocrystalline ZnO powders under irradiation of UV-C light, Sep. Purif. Technol. 58 (2007) 91–98, doi: 10.1016/j.seppur.2007.07.016.

[39] J. Fenoll, P. Flores, P. Hellín, C.M. Martínez, S. Navarro, Photodegradation of eight miscellaneous pesticides in drinking water after treatment with semiconductor materials under sunlight at pilot plant scale, Chem. Eng. J. 204–206 (2012) 54–64, doi: 10.1016/j.cej.2012.07.077.

[40] S. Ahmed, M.G. Rasul, R. Brown, M.A. Hashib, Influence of parameters on the heterogeneous photocatalytic degradation of pesticides and phenolic contaminants in wastewater: A short review, J. Environ. Manage. 92 (2011) 311–330, doi: 10.1016/j.jenvman.2010.08.028.

[41] J. Blanco, S. Malato, P. Fernández, A. Vidal, Compound parabolic concentrator technology development to commercial solar detoxification applications, Sol. Energ. 67 (1999) 317–330.

[42] Q.-S. Liu, T. Zheng, P. Wang, J.-P. Jiang, N. Li, Adsorption isotherm, kinetic and mechanism studies of some substituted phenols on activated carbon fibers, Chem. Eng. J. 157 (2010) 348–356, doi: 10.1016/j.cej.2009.11.013.

[43] K. Mohanty, D. Das, M.N. Biswas, Adsorption of phenol from aqueous solutions using activated carbons prepared from *Tectona grandis* sawdust by $ZnCl_2$ activation, Chem. Eng. J. 115 (2005) 121–131, doi: 10.1016/j.cej.2005.09.016.

[44] T.-T. Lim, P.-S. Yap, M. Srinivasan, A.G. Fane, $TiO_2$/AC composites for synergistic adsorption-photocatalysis processes: Present challenges and further developments for water treatment and reclamation, Crit. Rev. Environ. Sci. Technol. 41 (2011) 1173–1230, doi: 10.1080/10643380903488664.

[45] Y.A. Shaban, M.A. El Sayed, A.A. El Maradny, R.K. Al Farawati, M.I. Al Zobidi, Photocatalytic degradation of phenol in natural seawater using visible light active carbon modified (CM)-n-$TiO_2$ nanoparticles under UV light and natural sunlight illuminations, Chemosphere 91 (2013) 307–313, doi: 10.1016/j.chemosphere.2012.11.035.

[46] Ö. Kartal, M. Erol, H. Oğuz, Photocatalytic destruction of phenol by $TiO_2$ powders, Chem. Eng. 24 (2001) 645–649.

[47] H. El-Kamah, A. Tawfik, M. Mahmoud, H. Abdel-Halim, Treatment of high strength wastewater from fruit juice industry using integrated anaerobic/aerobic system, Desalination 253 (2010) 158–163, doi:10.1016/j.desal.2009.11.013.

[48] F. El-Gohary, A. Tawfik, U. Mahmoud, Comparative study between chemical coagulation/precipitation (C/P) versus coagulation/dissolved air flotation (C/DAF) for pre-treatment of personal care products (PCPs) wastewater, Desalination 252 (2010) 106–112, doi: 10.1016/j.desal.2009.10.016.

[49] I. Carra, E. Ortega-Gómez, L. Santos-Juanes, J.L. Casas López, J.A. Sánchez Pérez, Cost analysis of different hydrogen peroxide supply strategies in the solar photo-Fenton process, Chem. Eng. J. 224 (2013) 75–81, doi: 10.1016/j.cej.2012.09.067.

[50] L. Santos-Juanes Jordá, M.M. Ballesteros Martín, E. Ortega Gómez, A. Cabrera Reina, I.M. Román Sánchez, J.L. Casas López, J.A. Sánchez Pérez, Economic evaluation of the photo-Fenton process. Mineralization level and reaction time: The keys for increasing plant efficiency, J. Hazard. Mater. 186 (2011) 1924–1929, doi: 10.1016/j.jhazmat.2010.12.100.

[51] M. Molinos-Senante, F. Hernández-Sancho, R. Sala-Garrido, Economic feasibility study for wastewater treatment: A cost-benefit analysis, Sci. Total Environ. 408 (2010) 4396–4402, doi: 10.1016/j.scitotenv.2010.07.014.

[52] I. Muñoz, S. Malato, A. Rodríguez, X. Domènech, Integration of environmental and economic performance of processes. Case study on advanced oxidation processes for wastewater treatment, J. Adv. Oxid. Technol. 11 (2008) 270–275.